Evaluating chemical reactions upon seasonal heat storage in Danish geothermal reservoirs

Hanne Dahl Holmslykke and Claus Kjøller [1], Ida Lykke Fabricius[2]

[1] Department of Geochemistry, Geological Survey of Denmark and Greenland, Øster Voldgade 10, DK-1350 Copenhagen K, Denmark

[2] Department of Civil Engineering, Technical University of Denmark, Brovej 118. DK-2800 Kgs. Lyngby, Denmark

hdh@geus.dk

Keywords: High-temperature aquifer thermal energy storage, Deep aquifer thermal energy storage, Reactive transport modelling, Flooding experiments, Gassum Formation, Bunter Sandstone Formation.

ABSTRACT

In this study, two sets of core flooding experiments were performed at reservoir conditions and temperatures up to 150°C to investigate the effect of heating on geochemical processes when cores from two potential Danish geothermal reservoirs are flushed with synthetic brine at elevated temperature. The interpretation of geochemical effects caused by the introduction of heated formation water is supported by petrographic analysis of the cores prior to and after the flooding experiments and by geochemical modelling. Samples from the Lower Triassic Bunter Sandstone Formation and from the Upper Triassic – Lower Jurassic Gassum Sandstone Formation were tested. For the calcium carbonate containing Bunter Sandstone formation, the experiments were performed with Ca-depleted synthetic formation water to avoid loss of injectivity by calcium carbonate scaling at elevated temperatures. The results show that heating induced a series of silica dissolution/precipitation processes for both sandstones, including dissolution of quartz, weathering of Na-rich feldspar to kaolinite, replacement of plagioclase with albite and precipitation of muscovite. These processes are not expected to significantly deteriorate the reservoir physical properties. However, for the Bunter Sandstone formation, flushed with Ca-depleted brine, a significant portion of the cementing calcium carbonate dissolved. In the reservoir, this may ultimately reduce the mechanical strength of the geological formation. Thus, the study suggests that heat storage in geothermal reservoirs can be technically feasible in typical Danish geothermal sandstone reservoirs. However, in reservoirs containing calcium carbonate, means for avoiding calcium carbonate precipitation during heat storage should be chosen with caution to minimise possible reservoir damaging side effects.

1. INTRODUCTION

To overcome the temporal incongruity between the supply and demand for heat, seasonal storage of surplus heat in Danish geothermal reservoirs is considered. During summer, formation water is extracted from the reservoir and heated using excess heat, e.g. from power generation, prior to reinjection of the hot water into the reservoir. During winter, the stored hot water is extracted and used for district heating. The relatively high temperature of the geothermal reservoirs is considered to minimise the heat loss during storage in these reservoirs. Additionally, the lifetime of the geothermal reservoir may be extended as the heat storage increases the heat potential in the geothermal reservoir (Kabus et al., 2005; Réveillère et al., 2013).

Raising the temperature of the reservoir may, however, damage the reservoir e.g. through dissolution/precipitation processes and/or fines migration leading to reduced injectivity. In this study, two sets of core flooding experiments are conducted at reservoir conditions and temperatures up to 150°C to investigate the effect of heating on geochemical processes when cores from two potential Danish geothermal reservoirs are flushed with synthetic brine. The interpretation of geochemical effects caused by injection of heated formation water is supported by petrographic analysis of the cores prior to and after the flooding experiments and by geochemical modelling. Samples from the Lower Triassic Bunter Sandstone Formation and from the Upper Triassic – Lower Jurassic Gassum Sandstone Formation are tested. For the calcium carbonate containing Bunter Sandstone formation, the geochemical experiments are performed with Ca-depleted synthetic formation water in order to avoid loss of injectivity by calcium carbonate scaling at elevated temperatures. Parts of the experiments were recently published elsewhere (Holmslykke et al., 2017).

2. MATERIALS AND METHODS

2.1 Sample Description and Fluid

Two cylindrical specimens were prepared from a cored interval of the Upper Triassic – Lower Jurassic Gassum Formation in the Stenlille-2 well and one specimen from a cored interval of the Lower Triassic Bunter Sandstone Formation in the Tønder-3 well (Figure 1).

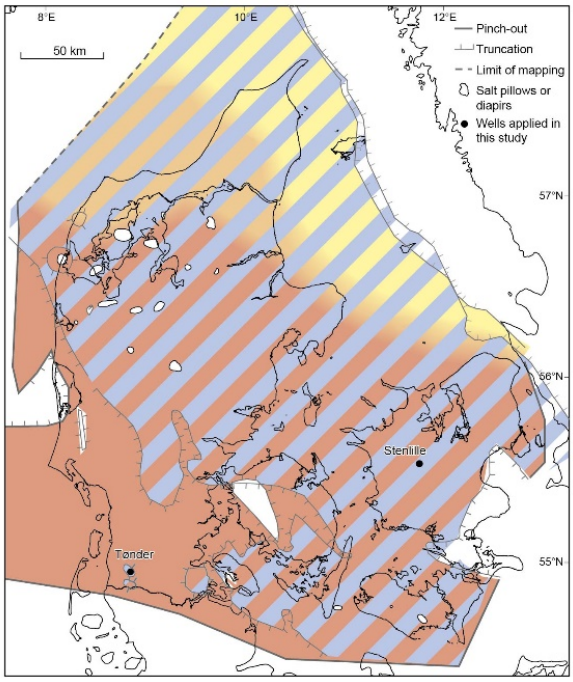

Figure 1: Map of Denmark showing the extent of the Gassum Sandstone Formation in blue colour and the Bunter Sandstone Formation in red colour (to the left) and the location of the Stenlille-2 well and Tønder-3 well where samples for this study were collected. Modified from Weibel et al. (2017).

The specimen of the Bunter Sandstone Formation represents the upper part of the upper Bunter sand unit and special care was taken to avoid sampling from the part of the upper Bunter sand unit containing cementing halite (Laier and Nielsen, 1989). All tested samples had the approximate length and diameter of 74.5 mm and 38.0 mm. Other pre test core data for the samples are shown in Table 1.

Table 1: Pre-test core data for the specimens used in this study.

Formation	Depth (m)	Temp. (°C)	Φ (%)	K_g (mD)
Gassum ($S_{0.05}$)	1539.5	50	29.11	195
Gassum ($S_{0.1}$)	1539.5	50	28.85	181
Bunter	1654.69	75	28.17	251

To evaluate the mineralogical composition of the Gassum and the Bunter Sandstone Formation at the tested depths, QEMSCAN® analyses of samples from the Gassum (1539.0 m) and the Bunter (1654.77 m) Sandstone Formations were performed. The Gassum Sandstone primarily consists of quartz (72 % (v/v)) and secondarily of feldspar (8% (v/v) K-feldspar and 2.5% (v/v) Na-feldspar) with minor contributions from kaolinite, mica, siderite and heavy minerals. Calcite is not detected in the sample from the Gassum Formation.

The Bunter Sandstone consists primarily of quartz (34% (v/v)) and secondarily of albite (12% (v/v)), K-feldspar (9% (v/v)), calcite (5% (v/v)), plagioclase (4% (v/v)), mixed layer clays (4% (v/v)), with minor contributions from illite, muscovite, carbonates and heavy minerals.

The chemical composition of the Gassum and the Bunter synthetic brines was modified from Laier (2008) (Table 2). Due to a high concentration (4500 mg/L) of aqueous calcium measured in the Bunter brine a softening of the formation water prior to reinjection in the reservoir may be necessary to prevent scaling problems in a heat storage facility. To simulate a situation with softening of the water, calcium was replaced by potassium in the synthetic brine.

Table 2: Chemical composition of the synthetic brines used in this study.

Element		Gassum	Bunter
Na	(mg/L)	59,000	99,987
K	(mg/L)	1,100	10,584
Mg	(mg/L)	1,600	1,900
Ca	(mg/L)	11,500	-
Sr	(mg/L)	600	-
Cl	(mg/L)	116,329	168,574
HCO_3^-	(mg/L)	80	12
SO_4^{2-}	(mg/L)	30	900
Salinity	(%)	17	23

2.3 Experimental Procedure

In all, three core flooding experiments were performed such that one experiment was performed with each of the two specimens from the Gassum Formation and one experiment with the specimen from the Bunter Sandstone Formation. Test conditions are shown in Table 3.

A brine saturated specimen was placed inside a Viton sleeve inside a hydrostatic core holder and in situ pressure was applied. Synthetic formation brine was used as the flooding fluid, and tests were performed at 23°C, reservoir temperature (50°C for the Gassum samples and 75°C for the Bunter sample), 100°C and 150°C allowing flow for minimum one week at each temperature. Downstream the core holder, effluent brine was collected for chemical analysis and cooled quickly (<5 min) to 23°C at high pressure. Subsequently, sample pressure was decreased to atmospheric pressure. The alkalinity and pH were measured immediately after sampling on unfiltered samples. The alkalinity was determined by Gran-titration (Stumm and Morgan, 1981). The rest of the sample was filtered through a 0.22 µm cellulose-acetate syringe filter into three separate polyethylene vials. Samples for cation and silicium analysis received 1 vol% of 7M HNO_3 and 10 vol% of 5M NaOH, respectively, and were kept refrigerated until ICP-MS analysis (PerkinElmer Elan6100DRC Quadrupol) with a standard deviation of 3-15% depending on the element measured. Samples for anion analysis (chloride

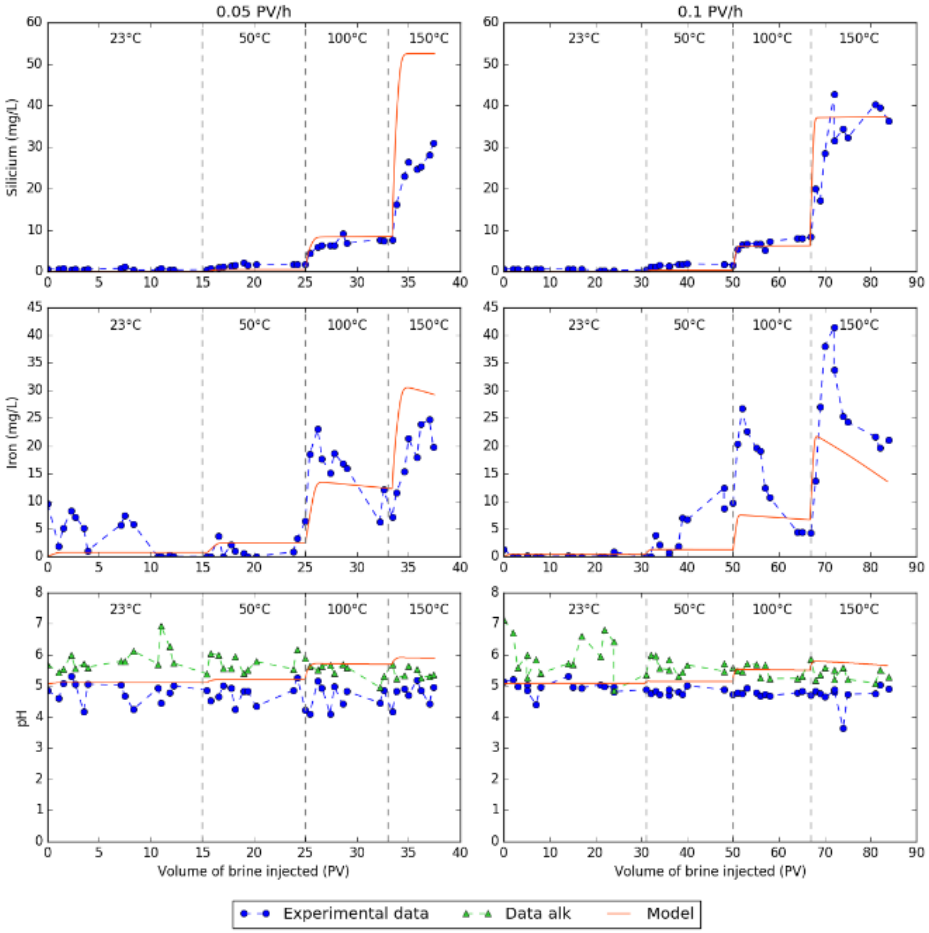

Figure 2: Measured and modelled silicium and iron concentration in the effluent of a Gassum Formation column flushed with synthetic Gassum brine at 23°C, 50°C (reservoir temperature), 100°C, and 150°C and with a flow velocity of 0.05 PV/h and 0.1PV/h. The model includes kinetically controlled dissolution/precipitation of albite, kaolinite, quartz and siderite (Holmslykke et al., 2017).

and sulphate) were frozen until ion-chromatography analysis (LC50-CD50, Dionex, CA, USA) with a quantification limit of 0.05 mg/L.

Table 3: Experimental test conditions.

Formation	Flow rate (PV/h)	Flow rate (cm/h)	Conf. pressure (bar)	Pore pressure (bar)
Gassum ($S_{0.05}$)	0.05	0.014	275	170
Gassum ($S_{0.1}$)	0.1	0.029	275	170
Bunter	0.05	0.014	315	180

Mineralogical changes in the specimens were identified by thin section analyses using optical microscope and backscatter electron microscopy prior to and after the flooding experiments to identify major chemical reactions responsible for the observed changes in aqueous chemistry. The mineralogical observations provide information for the geochemical modelling

2.3 Geochemical modelling

The injection of heated formation water into the geothermal reservoirs was modelled using the 1D reactive transport code PHREEQC version 3.0 (Parkhurst and Appelo, 2013). A 1D transport model column, comprising 10 cells with a length of 0.0745 m each, was constructed and flushed with synthetic formation water (Table 2) at 23°C, reservoir temperature (50°C for the Gassum samples and 75°C for the Bunter sample), 100°C and 150°C and at 170 bar or 180 bar pressure, respectively. Dispersion was not taken into account in the model. The thermodynamic data from the Thermoddem database (Blanc, 2017) were used since this database is optimised to high temperatures and includes a large range of silica minerals. The geochemical model was fitted to the experimental data from the 0.1PV/h experiment and subsequently tested against the results of the 0.05 PV/h experiment.

3. RESULTS AND DISCUSSION

3.1 Gassum Formation

For the Gassum Formation, mainly increases in the concentrations of aqueous silicium and iron were observed upon increasing the temperature (Figure 2). For Si, a constant level of silicium in the effluent was observed at each temperature for temperatures up to 100°C. Different flowrates created identical levels of Si concentration.

In general, the iron concentration peaked immediately after the temperature was increased. Subsequently, a decreasing iron concentration was observed. Tests with the ferrozine method showed that the iron is present as Fe(II) indicating no or only limited intrusion of oxygen to the samples.

No observable changes were identified for the concentration of chloride, sulphate, potassium, calcium, magnesium and sodium, probably due to the very high content of these elements in the synthetic brine and the relatively small changes that any reaction would cause. Aluminium remains below detection limit (0.03 mg/L) throughout the experiments (data not shown). The measured pH is relatively constant between 5 and 6 at all temperatures. An accurate pH measurement was difficult to obtain, since the pH drifted considerably during measurements. Therefore, both pH measured immediately after sampling and pH at the beginning of the alkalinity measurement are shown in Figure 2.

The petrographic analysis of the cores prior to and after the flooding experiments suggests that the Na-rich part of the feldspars is partly degraded in the cores, and that this process may well have been promoted by the flooding experiment. Furthermore, the flooding caused dissolution of siderite, whereas quartz appeared unaffected by the experiment.

Based on the observed mineralogical changes as well as the observed changes in the aqueous concentrations during the experiments, the geochemical model was fitted to the experimental data. A model including the minerals albite (as a proxy for Na-rich feldspar), kaolinite, quartz and siderite predicts the concentration of measured silicium and iron as well as the pH reasonably well for both experiments with the model optimised for the 0.1 PV/hr experiment (Figure 2).

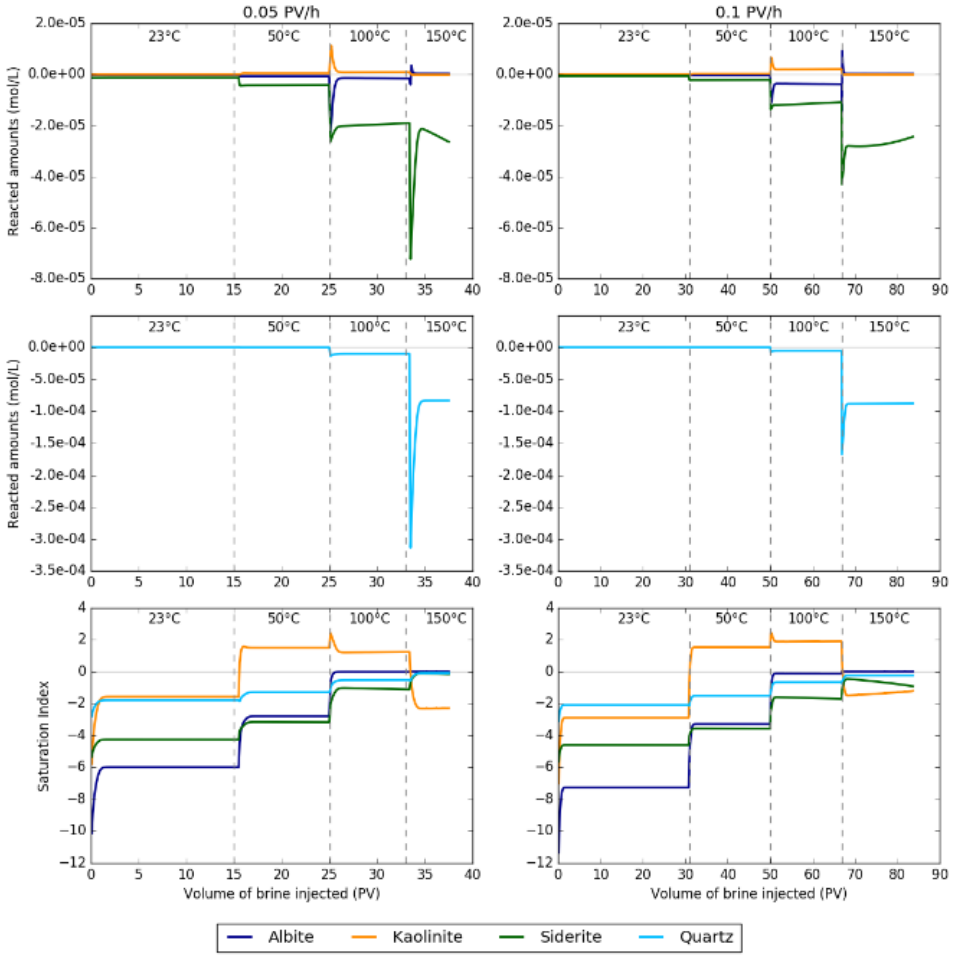

Figure 3: Reacted amounts and the Saturation Index for minerals included in a PHREEQC transport model of synthetic Gassum brine through a column in which kinetically controlled dissolution or precipitation of albite, kaolinite, siderite and quartz is allowed at 0.05 PV/h and 0.1 PV/h. A positive "Reacted amounts" indicates that the mineral precipitates, while a negative value indicates dissolution of the mineral. (Holmslykke et al., 2017)

Furthermore, in accordance with the measured aluminium concentrations, the model predicts the aqueous aluminium concentration to be 0.01 to 0.06 mg/L and thus near the detection limit (0.03 mg/L). Even though quartz dissolution was not identified by the petrographic analysis, the reaction was necessary to include in the model in order to reach the high silicium concentrations measured, especially at 150°C.

Confirming the petrographic analysis, the model results show that at reservoir conditions (50°C) dissolution of Na-rich feldspar and precipitation of kaolinite occurs (Figure 3). Weathering of Na-feldspar to kaolinite can be illustrated by the following reaction:

Feldspar

$$NaAlSi_3O_8 + H^+ + 0.5H_2O \rightarrow$$

Kaolinite

$$0.5Al_2Si_2O_5(OH)_4 + Na^+ + 2SiO_2(aq)$$

When the temperature increases to 100°C, the conversion of feldspar to kaolinite increases (Figure 3) as a result of an increased rate for both dissolution of feldspar and precipitation of kaolinite. The increasing temperature causes the solution to approach saturation with respect to albite (Figure 3), although even at 100°C equilibrium is not reached. The simulated saturation indices for albite at 100°C are -0.66 and -0.02 for the 0.1 PV/hr and 0.05 PV/hr experiment, respectively. In general, simulated negative saturation indices for temperatures ≤100°C indicate that the aqueous silicium concentration is not controlled by equilibrium with any of the silicium containing minerals. The close to constant aqueous silicium concentration obtained at each temperature step, apparently independently of the flow velocity (Figure 2) suggests that the silicium concentration is controlled by a quasi-stationary state between feldspar dissolution and kaolinite precipitation. The flow rate affects the magnitude of the dissolution/precipitation processes in this quasi-stationary state. Thus, at 100°C more feldspar is dissolved and kaolinite precipitated at the higher flow as compared to the lower flow rate due to a lower saturation index in the first case.

With increasing temperature, dissolution of quartz becomes increasingly important in the simulation, and at 100°C the dissolution of quartz is in the same order of magnitude as the dissolution of Na-feldspar. At 150°C, the dissolution of quartz increases sharply resulting in a significant increase in the aqueous silicium concentration (Figures 2 and 3). Thus, at 150°C quartz dissolution becomes the predominant process, completely suppressing the dissolution of feldspar and thereby the precipitation of kaolinite (Figure 3). This is in good agreement with several previous studies showing that dissolution of quartz increases sharply at elevated temperatures (Azaroual and Fouillac, 1997; Gong et al., 2012; Perlinger et al., 1987).

Figure 3 shows that simulated results follow the trend in the observed data with an immediate increase in the iron concentration upon temperature increase, then followed by a decrease in the iron concentration. However, the models seem to underestimate the iron concentration somewhat, in particular in the 0.1 PV/hr experiment. Thus, other sources than siderite may contribute to the aqueous iron concentrations observed in the core flooding experiments. One such source could be biotite. However, including biotite in the model has shown not to increase the iron concentration significantly. Release of iron due to corrosion of the equipment is unlikely since high corrosion-resistant Hastelloy®(C-276) was used in the experimental setup.

3.2 Bunter Sandstone Formation

For the Bunter Sandstone Formation, the most significant changes in the aqueous concentrations caused by injection of the Ca-depleted brine were increases in the aqueous concentration of calcium and silicium (Figure 4). Magnesium, on the other hand, shows a decreasing concentration when increasing the temperature to 100°C, and particularly to 150°C. No observable changes were identified for the concentration of chloride, sulphate, potassium, and sodium. Aluminium remains below detection limit (0.03 mg/L) throughout the experiments (data not shown).

The petrographic analysis of the Bunter Sandstone Formation prior to and after flooding with Ca-depleted brine suggests that while quartz and biotite do not show any obvious signs of chemical dissolution or precipitation, the Na-rich feldspars appears dissolved to some degree in both the unflushed and the flushed sample. Contrarily, K-rich feldspars show no signs of dissolution. Euhedral albite apparently grows in the pore space in the flushed samples. Dissolution of calcite occurs and all flushed samples also contain euhedral dolomite crystals.

As the source of aluminium for the observed precipitation of albite remains unclear from the petrographic analysis, equilibrium calculations using PHREEQC were performed focusing on the equilibrium state of feldspars in the effluent of the flooding experiment. The model shows that dissolution of any of the alkali feldspars is not likely to occur during the flooding experiment. In contrast, the plagioclase may potentially dissolve during the experiment.

The best fit of the model to the experimental data was obtained by kinetically controlled dissolution or precipitation of calcite, dolomite, albite, plagioclase in the reactive transport model. As the exact chemical composition of the plagioclase remains unknown, a plagioclase with 30% albite is included in the model.

Quartz dissolution was also included in the model in accordance with the findings from the Gassum Formation experiment (Holmslykke et al., 2017). Stability diagrams for K-feldspar and its weathering

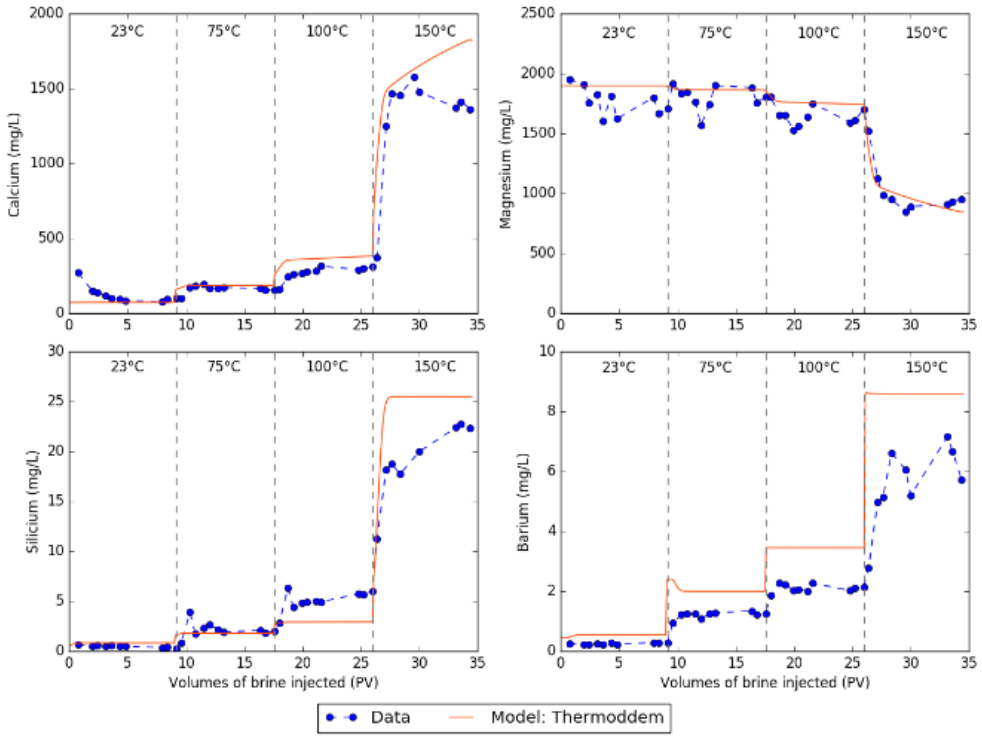

Figure 4: Measured and modelled calcium (top left), magnesium (top right), silicium (bottom left) and barium (bottom right) concentrations in the effluent of a Bunter Sandstone Formation sample flushed with calcium depleted synthetic formation water (Table 2) with a flow velocity of 0.05 PV/h and at 23, 75 (reservoir temperature), 100 and 150°C.

products suggest that muscovite may be the stable weathering product in the experiment due to the high potassium concentration in the modified Bunter brine, and therefore muscovite was also included in the model. Finally, equilibrium with barite was imposed in the model due to the presence of barite in the samples.

Figure 4 shows the results of the geochemical simulation together with the experimental data for the flooding experiment. The measured concentrations of calcium, magnesium, silicium and barium are predicted reasonably well for the optimised model. Furthermore, in accordance with the measured aluminium concentrations, the model predicts the aqueous aluminium concentration to be close to the detection limit (0.03 mg/L; data not shown).

According to our model, the calcium concentration is controlled by equilibrium with calcite ($CaCO_3$), while the magnesium concentration is kinetically controlled by precipitation of dolomite ($CaMg(CO_3)_2$) (Figure 5). Despite super saturation with respect to dolomite (SI = 1.6) at temperatures up to 75°C, no or only unmeasurable amounts of dolomite precipitate, and dolomite precipitation only occurs at temperatures ≥100°C. Thus, at temperatures ≥100°C the heating induces dolomitisation. Dolomitisation where calcite dissolution and dolomite precipitation occur in a 1:1 molar ratio as indicated by the experimental data, can be illustrated by the following equation:

$$2CaCO_3(s) + Mg^{2+}(aq) \rightarrow CaMg(CO_3)_2(s) + Ca^{2+}(aq)$$

where the subindices s and aq represent solid and aqueous phases, respectively.

Dolomitisation depends on specific conditions which include a supply of aqueous solution with high Mg/Ca ratio; elevated temperature and high degree of supersaturation (Banerjee, 2016); all of which are fulfilled in the present study. An increase in the Mg/Ca ratio of the solution increases the free energy of the dolomitisation reaction and therefore increases the rate. The strong dependence of dolomite precipitation rate on temperature (Al-Helal et al., 2012; Arvidson and Mackenzie, 1999; Chen et al., 2004; Jones and Xiao, 2005; Merino and Canals, 2011; Sibley et al., 1994; Wilson et al., 1990) is due to the high activation energies found for very High-Mg Calcite and dolomite (48 and 49-50 kcal/mol, respectively (Katz and Matthews, 1977)) compared to the approximately 10 kcal/mol activation energy for calcite precipitation (Arvidson and Mackenzie, 1999).

The lack of dolomite formation at low temperatures in solutions that were supersaturated with respect to dolomite (Land, 1998; Sibley et al., 1994) and also in recent and geologically relatively young marine carbonate environments (Machel, 2004) is typically explained by a long induction time during the dolomitisation formation process. In these solutions, dolomite might have nucleated but the reaction might still be in the induction period and therefore no products were detected.

Due to the high sulphate concentration in the Bunter brine, the role of sulphate as a potential kinetic inhibitor to dolomitisation deserves special attention. The presence of even small amounts of sulphate has been shown to inhibit dolomite formation (Baker and Kastner, 1981; Morrow and Ricketts, 1988) by formation of a layer of $CaSO_4$ on the calcite surface and by slowing the rate of calcite dissolution as the degree of calcite subsaturation correlates inversely with the sulphate concentration. Other studies show that the amount of dissolved sulphate has no influence on the rate of dolomitisation (Morrow and Ricketts, 1986) or may even promote dolomitisation. Thus, dolomite formation in sulphate rich solutions has been explained by dolomite growth through the adsorption of Mg-sulphate complexes (Brady et al., 1996). In our case, sulphate inhibition does not seem to take place as the simulated results correspond well with the observed concentrations of Ca and Mg without introducing inhibition in the numerical model.

The model also reproduces the measured silicium concentration reasonably well (Figure 4) as well as the aluminium concentration which is below the detection limit. The silicium concentration is controlled by equilibrium with albite at all the tested temperatures (Figure 6). However, the concentration level is determined by the strong coupling with the kinetically controlled dissolution and precipitation of silica minerals. Thus, at reservoir conditions (75°C) the silicium concentration is controlled by dissolution of small amounts of albite and precipitation of small amounts of muscovite. The precipitation of muscovite may very well be facilitated by the increased potassium concentration in the injected modified brine leading to a fluid super saturated with respect to muscovite as albite dissolves. Upon a temperature increase to 100°C, dissolution of quartz along with conversion of small amounts of plagioclase to albite is observed while precipitation of muscovite continues. At 150°C both the dissolution of quartz and the albitisation increases.

Albitisation of plagioclase may be described by a reaction such as:

Plagioclase

$$Na_{0.7}Ca_{0.3}Al_{1.3}Si_{2.7}O_8 + 0.3Na^+ + 0.3H_4SiO_4 \rightarrow$$

Albite

$$NaAlSi_3O_8 + 0.3Ca^{2+} + 0.3Al^{3+} + 1.2OH^-$$

The process involves the supply of sodium and silicium, while calcium and aluminium are released to the solution. In our experiment, the supply of sodium is ensured through the injected water (Table 1), whereas the supply of silicium is facilitated by dissolution of quartz (Figure 8). The release of calcium due to albitisation is insignificant compared to the release of calcium due to calcite dissolution (Figures 5 and 6). The significant release of calcium due to calcite dissolution may in fact inhibit the precipitation of albite. Even though aluminium is released to the solution by the albitisation, the aluminium concentration remains below the detection limit due to precipitation of muscovite. Thus, while the silicium concentration is controlled by equilibrium with albite, the plateau reached at each temperature is affected by a strong coupling between the processes of quartz dissolution, albitisation, calcite dissolution and muscovite precipitation.

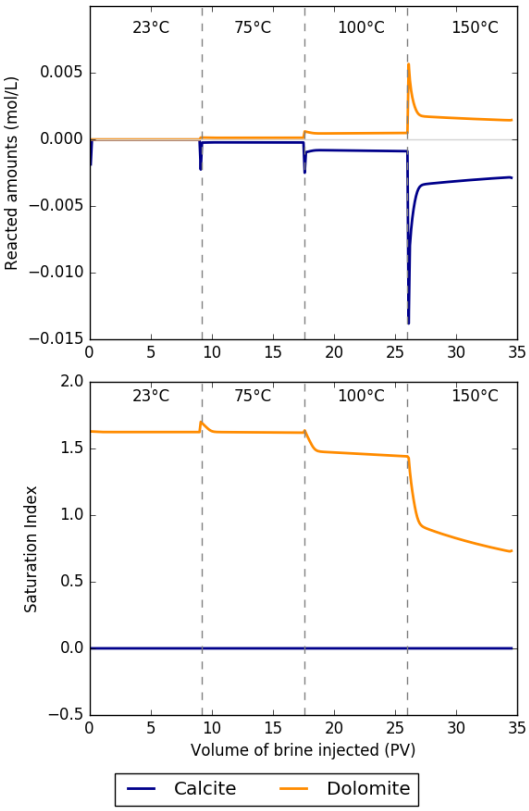

Figure 5: Reacted amounts (top) and Saturation Index (bottom) for calcite and dolomite calculated in a PHREEQC reactive transport model where synthetic Bunter brine (Table 2) is flushed through a column in which kinetically controlled dissolution or precipitation of calcite, dolomite, plagioclase, quartz, albite and muscovite is allowed. A positive "Reacted amounts" indicates that the mineral precipitates, while a negative value indicates dissolution of the mineral.

Dissolution of quartz is quantitatively the most important process (Figure 6). It is well known that the solubility of quartz as well as the dissolution rate increases with increasing temperature (Rimstidt and Barnes, 1980). Especially at temperatures above 100°C, the rate of quartz dissolution increases significantly (Figure 6) as also observed in the experiments with the Gassum Sandstone (Holmslykke et al., 2017). This increases the supply of silicium for the albitisation, thereby pushing equation (2) to the right, resulting in an enhancement of the albitisation at 150°C.

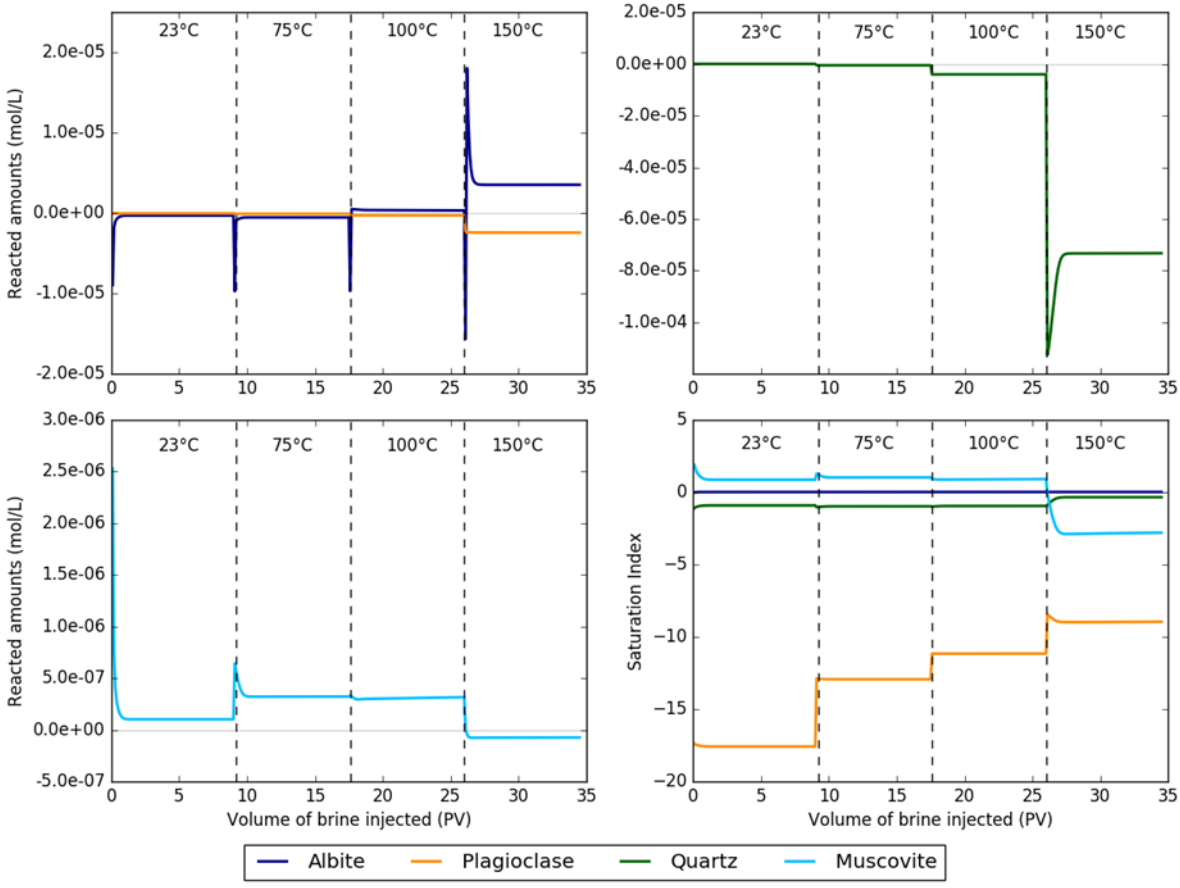

Figure 6: Reacted amounts (top) and Saturation Index (bottom) for silica minerals calculated in a PHREEQC reactive transport model where synthetic Bunter brine (Table 2) is flushed through a column in which kinetically controlled dissolution or precipitation of calcite, dolomite, plagioclase, quartz, albite and muscovite (Table 3) is allowed. A positive "Reacted amounts" indicates that the mineral precipitates, while a negative value indicates dissolution of the mineral.

3. CONCLUSIONS

Although heating induced a series of silica dissolution/precipitation processes for both sandstones, including dissolution of quartz, weathering of Na-rich feldspar to kaolinite, replacement of plagioclase with albite and precipitation of muscovite, these processes are not expected to significantly deteriorate the reservoir physical properties. However, for the Bunter Sandstone Formation, that was flushed with Ca-depleted brine, a significant portion of the cementing calcium carbonate dissolved. In the reservoir, this may ultimately reduce the mechanical strength of the geological formation with a risk of decreasing the bore hole stability. Thus, the study suggests that heat storage in geothermal reservoirs can be technically feasible in typical Danish geothermal sandstone reservoirs. However, in reservoirs containing calcium carbonate, means for avoiding calcium carbonate precipitation during heat storage should be chosen with caution in order to minimise possible reservoir damaging side effects.

REFERENCES

Al-Helal, A.B., Whitaker, F.F. and Xiao, Y. Reactive transport modeling of brine reflux: dolomitization, anhydrite precipitation, and porosity evolution. J. Sediment. Res. 82, (2012) 196-215.

Arvidson, R.S. and Mackenzie, F.T. The dolomite problem; control of precipitation kinetics by temperature and saturation state. Am. J. Sci. 299, (1999), 257-288.

Azaroual, M. and Fouillac, C. Experimental study and modelling of granite-distilled water interactions at 180 degrees C and 14 bars. Appl. Geochem. 12, (1997), 55-73.

Baker, P.A. and Kastner, M. Constraints on the formation of sedimentary dolomite. Science 213, (1981), 214-216.

Banerjee, A. Estimation of dolomite formation: Dolomite precipitation and dolomitization. J. Geol. Soc. India 87, (2016), 561-572.

Blanc P. Thermoddem : Update for the 2017 version. Report BRGM/RP-66811-FR, 20 pp. (2017).

Brady, P.V., Krumhansl, J.L. and Papenguth, H.W. Surface complexation clues to dolomite growth. Geochim. Cosmochim. Acta 60, (1996), 727-731.

Chen, D., Qing, H. and Yang, C. Multistage hydrothermal dolomites in the Middle Devonian (Givetian) carbonates from the Guilin area, South China. Sedimentology 51, (2004), 1029-1051.

Gong, Q., Deng, J., Han, M., Yang, L. and Wang, W. Dissolution of sandstone powders in deionised water over the range 50–350 °C. Appl. Geochem. 27, (2012), 2463-2475.

Holmslykke, H.D., Kjøller, C. and Fabricius, I.L. Core flooding experiments and reactive transport modeling of seasonal heat storage in the hot deep Gassum Sandstone Formation, Earth and Space Chemistry, 1, (2017), 251-260.

Jones, G.D. and Xiao, Y. Dolomitization, anhydrite cementation, and porosity evolution in a reflux system: Insights from reactive transport models. AAPG Bulletin 89, (2005), 577-60.

Kabus, F., Hofmann, F. and Möllmann, G. Aquifer storage of waste heat arising from a gas and steam cogeneration plant - concept and first operating experience, World Geothermal Congress 2005, Antalya, Turkey, (2005).

Katz, A. and Matthews, A. The dolomitization of CaCO3: an experimental study at 252–295°C. Geochim. Cosmochim. Acta 41, (1977), 297-308.

Laier, T. Chemistry of Danish saline formation waters relevant for core fluid experiments – Fluid chemistry data for lab experiments related to CO2 storage on deep aquifers. GEUS report 2008/48, Geological Survey of Denmark and Greenland, Copenhagen, (2008).

Laier, T. and Nielsen, B.L. Cementing halite in Triassic Bunter Sandstone (Tønder southwest Denmark) as a result of hyperfiltration of brines. Chem. Geol. 76, (1989), 353-363.

Land, L.S. Failure to precipitate dolomite at 25 °C from dilute solution despite 1000-fold oversaturation after 32 years. Aq. Geochem. 4, (1998)3, 61-368.

Machel, H.G. Concepts and models of dolomitization: a critical reappraisal. Geological Society, London, Special Publications 235, (2004), 7-63.

Merino, E. and Canals, À. Self-accelerating dolomite-for-calcite replacement: Self-organized dynamics of burial dolomitization and associated mineralization. Am. J. Sci. 311, (2011), 573-607.

Morrow, D.W. and Ricketts, B.D. Chemical controls on the precipitation of mineral analogues of dolomite: The sulfate enigma. Geology 14, (1986), 408-410.

Morrow, D.W. and Ricketts, B.D. Experimental investigation of sulfate inhibition of dolomite and its mineral analogues, in: Shukla, V., Baker, P.A. (Eds.), Sedimentology and Geochemistry of Dolostones. SEPM Special Publication, pp. 25-38, (1988).

Parkhurst, D.L. and Appelo, C.A.J. Description of input and examples for PHREEQC version 3 - A computer program for speciation, batch-reaction, one-dimensional transport, and inverse geochemical calculations, U.S. Geological Survey Techniques and Methods, (2013).

Perlinger, J.A., Almendinger, J.E., Urban, N.R. and Eisenreich, S.J. Groundwater geochemistry of aquifer thermal energy storage - Long term test cycle. Water Resour. Res. 23, (1987), 2215-2226.

Réveillère, A., Hamm, V., Lesueur, H., Cordier, E. and Goblet, P. Geothermal contribution to the energy mix of a heating network when using Aquifer Thermal Energy Storage: Modeling and application to the Paris basin. Geothermics 47, (2013), 69-79.

Rimstidt, J.D. and Barnes, H.L. The kinetics of silica-water reactions. Geochim. Cosmochim. Acta 44, (1980), 1683-1699.

Sibley, D.F., Nordeng, S.H. and Borkowski, M.L. Dolomitization kinetics of hydrothermal bombs and natural settings. J. Sediment. Res. 64, (1994), 630-637.

Stumm, W. and Morgan, J.J. Aquatic Chemistry, John Wiley, N. Y., (1981).

Weibel, R., Olivarius, M., Kristensen, L., Friis, H., Hjuler, M.L., Kjøller, C., Mathiesen, A. and Nielsen, L.H. Predicting permeability of low-enthalpy geothermal reservoirs: A case study from the Upper Triassic – Lower Jurassic Gassum Formation, Norwegian–Danish Basin. Geothermics 65, (2017), 135-157.

Wilson, E.N., Hardie, L.A. and Phillips, O.M. Dolomitization front geometry, fluid flow patterns, and the origin of massive dolomite; the Triassic Latemar buildup, northern Italy. Am. J. Sci. 290, (1990), 741-796.

Acknowledgements (optional)

This research was funded by the Danish Council for Strategic Research (now Innovation Fund Denmark) as part of the Heat Storage in Hot Aquifers (HeHo) project (Grant 10-093934).